Decomposition of in situ particulate absorption spectra

Alison Chase, Emmanuel Boss, Ronald Zaneveld, Annick Bricaud, Hervé Claustre, Josephine Ras, Giorgio Dall'Olmo, Toby K. Westberry

Methods in Oceanography 7 (2013) 110–124

Contents lists available at ScienceDirect

Methods in Oceanography

journal homepage: www.elsevier.com/locate/mio

Full length article

Decomposition of in situ particulate absorption spectra

Alison Chase [a,*], Emmanuel Boss [a], Ronald Zaneveld [b], Annick Bricaud [c], Herve Claustre [c], Josephine Ras [c], Giorgio Dall'Olmo [d], Toby K. Westberry [e]

[a] University of Maine, 5706 Aubert Hall, Orono, ME, 04469, USA
[b] WET Labs, Philomath, OR, 97370, USA
[c] LOV, Université P. et M. Curie-Paris 6 and CNRS, Villefranche-sur-Mer, France
[d] Plymouth Marine Laboratory, Prospect Place, Plymouth, PL1 3DH, UK
[e] Oregon State University, Corvallis, OR, 97331, USA

ARTICLE INFO

Article history:
Available online 12 March 2014

Keywords:
Bio-optics
Particulate absorption
Phytoplankton pigments
Spectral decomposition

ABSTRACT

A global dataset of in situ particulate absorption spectra has been decomposed into component functions representing absorption by phytoplankton pigments and non-algal particles. The magnitudes of component Gaussian functions, used to represent absorption by individual or groups of pigments, are well correlated with pigment concentrations determined using High Performance Liquid Chromatography. We are able to predict the presence of chlorophylls *a*, *b*, and *c*, as well as two different groups of summed carotenoid pigments with percent errors between 30% and 57%. Existing methods of analysis of particulate absorption spectra measured in situ provide for only chlorophyll *a*; the method presented here, using high spectral resolution particulate absorption, shows the ability to obtain the concentrations of additional pigments, allowing for more detailed studies of phytoplankton ecology than currently possible with in-situ spectroscopy.

* Corresponding author. Tel.: +1 603 731 3708.
E-mail address: alison.p.chase@maine.edu (A. Chase).

http://dx.doi.org/10.1016/j.mio.2014.02.002
2211-1220

1. Introduction

The absorption of light in the ocean is routinely used to infer the concentration of the absorbing constituents in seawater. The total particulate absorbing matter is composed of both phytoplankton and non-algal particles such as detritus and minerals. Different phytoplankton groups have evolved unique pigment assemblages for optimizing light absorption, both for photosynthetic and photoprotective purposes. These different pigment assemblages result in variations in phytoplankton absorption spectra, which can be used to characterize phytoplankton populations, for example based on pigment ratios (Mackey et al., 1996) or size classification algorithms (Uitz et al., 2006).

Extracting information about different pigments and phytoplankton groups from particulate absorption spectra is a challenging task that past studies have met with mixed success. Hoepffner and Sathyendranath (1991, 1993) and Lohrenz et al. (2003) used Gaussian functions to represent absorption by different chlorophyll and carotenoid pigments and decompose laboratory-measured phytoplankton absorption spectra. Other approaches include derivative analysis (Bidigare et al., 1989), discriminant analysis (Johnsen et al., 1994), neural networks (Bricaud et al., 2007), similarity algorithms (Millie et al., 1997; Kirkpatrick et al., 2000), and inverse modeling for extraction of pigment-specific absorption spectra (Moisan et al., 2011). However, in all of these past studies, laboratory measurements of phytoplankton absorption spectra have been used, either with phytoplankton cultures or with natural samples collected in situ. In this study, we use a Gaussian decomposition method to extract pigment information from particulate absorption spectra measured in situ; spectra are measured by pumping water through an instrument deployed on board and therefore water samples are not handled. In situ data can be obtained with high temporal and spatial resolution under highly variable environmental conditions, and thus provide a wide range of phytoplankton absorption spectra through both space and time.

2. Data and methods

2.1. Particulate absorption and pigment data

The spectral absorption data used in this work were measured with a WETLabs AC-S instrument, an in situ spectrophotometer that provides hyperspectral absorption and attenuation data in the range 400–750 nm with ~4 nm resolution (Moore et al., 1997; Rhoades et al., 2004). The spectral range and measurement wavelengths vary slightly between sensors and for a specific sensor following factory calibration. Several different AC-S instruments were used during the collection of spectral absorption in this study. The instruments were deployed using an in-line system that allows nearly continuous sampling of surface ocean water; details of the flow-through system are provided in Slade et al. (2010). Total absorption was measured on unfiltered bulk seawater, followed by 0.2 μm-filtered measurements for ten minutes every hour, or five minutes every half-hour in coastal waters. Particulate absorption data is obtained using a series of steps; after one-minute binning, 0.2 μm filtered data are interpolated to the time of the total measurement and are subtracted:

$$a_p(\lambda) = a_{tot}(\lambda) - a_{0.2\ \mu m}(\lambda) \quad (1)$$

where $a_p(\lambda)$ is particulate absorption, $a_{tot}(\lambda)$ is total absorption, and $a_{0.2\ \mu m}(\lambda)$ is the filtered fraction. The resulting $a_p(\lambda)$ spectra are then simultaneously corrected for small temperature differences between total and filtered measurements and for scattering using the proportional scattering correction (Slade et al., 2010). In the rare cases where the c-side lamp of the AC-S burned out mid-leg (~5% of match-up data points used in this study), a flat scattering correction was applied, similar to the correction used with laboratory spectrophotometers (Boss et al., 2013).

Five different AC-S sensors from four different labs (serial numbers 007, 043, 057, 082, 091) were used with the flow-through technique during the Tara Oceans expedition, a 2.5 year-long expedition from fall of 2009 to spring of 2012 along a 57,000 nautical miles oceanic route spanning the Indian, Atlantic and Pacific oceans (Karsenti et al., 2011). The particulate absorption data from Tara Oceans have been binned to one-minute temporal resolution. Data points with coincident HPLC data are selected from this one-minute binned dataset (hereafter "match-up points"); 87 of the 210 match-up

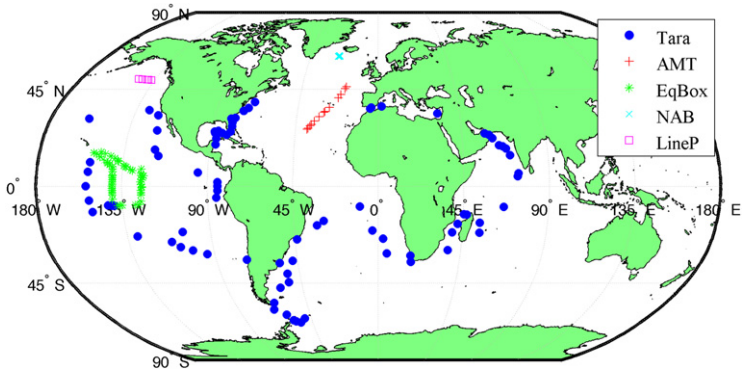

Fig. 1. Locations of the match-up points used to develop the method presented in this study, from five different expeditions. See Section 2.1 for a description of the expeditions. Data spans 2006–2012.

points used in this paper are from this Tara Oceans dataset. The Tara Oceans data are further binned to 1 km^2 resolution, resulting in 69,944 data points from across the globe. We apply our method, described below, to this 1 km^2 binned dataset after demonstrating the ability to detect pigments by decomposition of absorption spectra.

The Tara Oceans match-up points are combined with particulate absorption spectra and HPLC pigment information from four other expeditions. These expeditions are from the North Atlantic (19th Atlantic Meridional Transect, 2009, 17 match-up data points; North Atlantic Bloom Experiment, 2008, 33 match-up data points), Equatorial Pacific (2006, 67 match-up data points), and Subarctic Northeast Pacific (LineP, 2009, 6 match-up data points). These studies, described in Dall'Olmo et al. (2009) and Westberry et al. (2010), add spatial coverage to the Tara Oceans dataset and increase both the number of points and the dynamic range of absorption measurements and pigment concentrations used for development of the method presented here. The total number of match-up points from all five expeditions used in this study is 210 (Fig. 1).

Discrete water samples from all five expeditions were filtered and preserved for High Performance Liquid Chromatography (HPLC) pigment analysis. The Tara Oceans HPLC analysis was carried out according to the method described by Ras et al. (2008), adapted from Van Heukelem and Thomas (2001). Tara Oceans HPLC measurements used in the study are from the surface, defined as depth $\leq$5 m. Horn Point laboratories performed HPLC analysis for the other expeditions (Van Heukelem and Thomas, 2001; Hooker et al., 2009). To reduce noise in the data, the Tara Oceans AC-S one-minute binned spectra from 30 min before and after the HPLC sampling time were averaged together for comparison with pigment concentrations.

2.2. Correction for AC-S filter factors

Although the AC-S returns data at a resolution of $\sim$4 nm, the spectral bandwidth of individual filter steps ranges from 14 to 18 nm (Sullivan et al., 2006), resulting in a smoothing of the measured absorption spectra. These filter factors are applied automatically within the instrument, but can be corrected for to retrieve the "true" measured absorption spectrum. An iterative method is used to find the spectrum that most closely matches the original measured spectrum when convolved with the known filter functions (Appendix). The resulting "un-smoothed" spectra have slightly enhanced peaks and shoulders (Fig. 2), which increase the accuracy of the spectral decomposition method described below at some wavelengths of peak absorption.

2.3. Spectral decomposition

After we corrected the AC-S spectra for the effect of the filter factors, we decomposed each spectrum into component functions. Previous work by Hoepffner and Sathyendranath (1991)

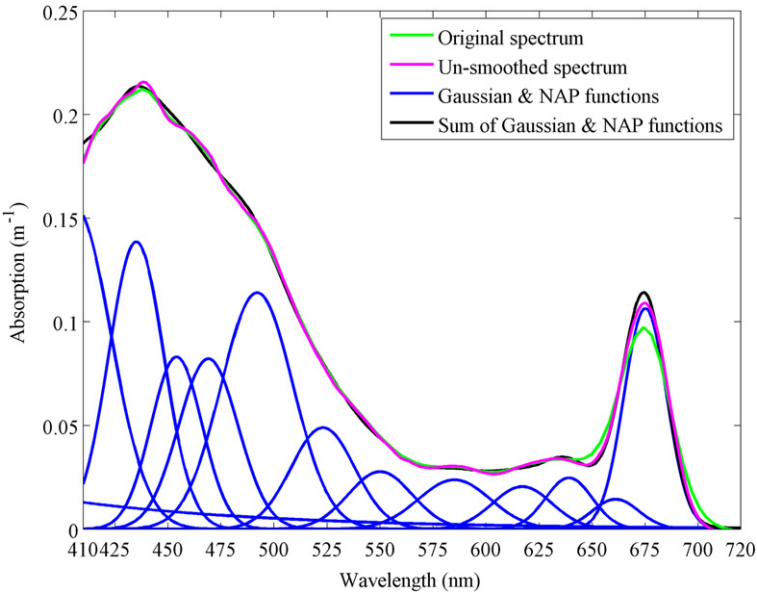

Fig. 2. Example of correction for filter factors ("Un-smoothed spectrum") and spectral decomposition, resulting in component Gaussian and non-algal particle (NAP) functions.

and others have found a Gaussian shape to be successful for modeling absorption by individual phytoplankton pigments, and twelve individual Gaussian functions are used in our study. In general, the fit will improve with the addition of more Gaussians; however, we have chosen the Gaussians to approximately represent the locations of peak absorption by different phytoplankton pigments, which allows us to investigate correlations with known pigment concentrations obtained from HPLC. In addition, we added a peak at 550 nm to represent absorption by the photosynthetic pigment phycoerythrin; although we do not have HPLC information for this pigment, we hope that future flow-cytometry and/or fluorescence data will be available to validate the presence of phycoerythrin-containing phytoplankton. Thus we use 11 Gaussian functions with peak locations associated with HPLC pigments and modeled after Hoepffner and Sathyendranath (1993) and Bricaud et al. (2004), and a 12th Gaussian function to represent phycoerythrin. In addition to the Gaussian functions representing absorption by phytoplankton pigments, absorption by non-algal particles ($a_{\mathrm{NAP}}(\lambda)$) is modeled using a decreasing exponential function (Iturriaga and Siegel, 1989). In total, thirteen functions spanning 410–720 nm are used in the spectral decomposition. The values 410 and 720 nm are chosen since all of the AC-S instruments used in the study have data that falls within these spectral limits.

We used the 210 match-up points to determine the center wavelengths and widths of the Gaussian functions by letting the initial values of these two parameters vary iteratively with bounds of ±5 nm (Table 1). We used a weighted least-squares inversion, and minimized the value of the cost function X^2:

$$X^2 = \sum_{\lambda=410}^{720} \frac{\left(a_{\mathrm{p}}(\lambda) - \left(\sum_{i=1}^{12} a_{\mathrm{gaus}}(\lambda_{\mathrm{i}}) \exp\left\{-0.5\left[\frac{\lambda-\lambda_{\mathrm{i}}}{\sigma_i}\right]^2\right\} + a_{\mathrm{NAP}}(400)\exp\{-0.01\,(\lambda-400)\}\right)\right)^2}{\sigma_{\mathrm{SD}}^2\,(\lambda)} \tag{2}$$

where $a_{\mathrm{p}}(\lambda)$ is the AC-S-measured particulate absorption spectrum, $a_{\mathrm{gaus}}(\lambda_i)$ denotes the magnitude of the ith Gaussian function, λ_i is the center wavelength of the ith Gaussian, σ_i is the width of the ith Gaussian, and $a_{\mathrm{NAP}}(\lambda)$ is the magnitude of absorption by non-algal particles. The equation is normalized by the standard deviation of the measured absorption spectra at each wavelength, denoted $\sigma_{\mathrm{SD}}^2(\lambda)$. The least-squares inversion was repeated for all 210 match-up points, and the means and

Table 1
Center wavelengths of Gaussian functions used as input for the iterative least-squares inversion ("Initial peak location"), and mean center wavelengths resulting from the inversion ("Final peak location"). Same definition for "Initial σ" and "Final σ"; σ is related to the full width half maximum (FWHM) by: FWHM $= \sigma * 2.355$. Standard deviations for both peak center wavelength and width are shown; $n = 210$. Abbreviations: Chl = chlorophyll; PPC = photoprotective carotenoids; PSC = photosynthetic carotenoids; PE = phycoerythrin.

Pigment(s)	Chl *a*&*c*	Chl *a*	Chl *b*&*c*	Chl *b*	PPC	PSC	PE	Chl *c*	Chl *a*	Chl *c*	Chl *b*	Chl *a*
Initial peak location (nm)	409	437	457	467	491	527	552	585	620	639	658	676
Final peak location (nm)	406	435	454	469	492	523	550	585	617	639	661	675
Peak std. dev. (nm)	±3.3	±2.4	±2.6	±2.1	±3.1	±2.6	±3.4	±3.6	±2.7	±2.7	±3.0	±1.7
Initial σ (nm)	15	15	15	15	15	15	15	15	15	15	15	15
Final σ (nm)	17	13	12	14	17	15	15	17	14	11	11	10
σ std. dev. (nm)	±3.8	±1.9	±1.9	±2.8	±1.7	±2.5	±2.6	±2.6	±2.9	±1.4	±1.5	±0.6

Table 2
Correlations between HPLC pigment concentrations and $a_{gaus}(\lambda_i)$ at ten different pigment absorption wavelengths. Correlation values are Spearman's rank correlation coefficient (non-parametric; denoted ρ). *A* and *B* are coefficients determined using Eq. (4) (Section 2.4).

Wavelength (nm)	Pigment(s)	ρ	*A*	*B*	e_{median} (%)
435	TChl *a*	0.868	0.031	0.578	35
617	TChl *a*	0.834	0.003	0.758	36
675	TChl *a*	0.899	0.014	0.798	30
454	0.03(TChl *b*) + 0.07(Chl *c*)	0.845	0.028	0.414	57
469	TChl *b*	0.783	0.066	0.533	52
661	TChl *b*	0.747	0.018	0.668	40
585	Chl *c*	0.846	0.014	0.582	53
639	Chl *c*	0.894	0.012	0.641	41
492	PPC	0.606	0.046	0.650	51
523	PSC	0.855	0.013	0.588	49

PPC = α-carotene + β-carotene + zeaxanthin + alloxanthin + diadinoxanthin.
PSC = 19′-hexanoyloxyfucoxanthin + fucoxanthin + 19′-butanoyloxyfucoxanthin + peridinin.
e_{median} = median relative error (%).

standard deviations of all center wavelengths and widths were calculated and used for subsequent analysis (Table 1). Using fixed values for center wavelengths and widths greatly reduces the time needed to execute the decomposition method, and standardizes the decomposition to all of the spectra, allowing for application of the method to a much larger spectral absorption dataset (e.g. Tara Oceans, ~70,000 1 km^2 binned absorption spectra).

Absorption by non-algal particles (NAP) is accounted for by the inclusion in Eq. (2) of an exponentially decaying NAP function:

$$a_{NAP}(\lambda) = a_{NAP}(400\ \text{nm}) * \exp(-0.01 * (\lambda - 400\ \text{nm})). \quad (3)$$

A sensitivity study of the value used for the slope of NAP absorption was conducted using exponent values ranging from -0.006 nm^{-1} to -0.013 nm^{-1}. The values of the relative median error (e_{median}, described in Section 2.4; values shown in Table 2) were found to vary by an average of 3%, with improvements in modeled phytoplankton absorption ($a_{gaus}(\lambda_i)$) as assessed by increased correlation with match-up data points found for some absorption peaks but not others. Thus, the value chosen for the NAP absorption slope does not strongly influence the results presented here. We spectrally weighted the decomposition by the inverse of the standard deviation associated with the particulate absorption spectra measurements at each wavelength ($\sigma^2_{SD}(\lambda)$, e.g. AC-S data have higher noise in the blue due to lower lamp output in that part of the spectrum). Note that for the Tara Oceans data, we have uncertainty values for each individual absorption spectrum, which are calculated as the standard deviations of the one-minute binned spectra. However, in the case of the other four expeditions, spectral uncertainty data was not available, so we used a mean uncertainty spectrum calculated from all the Tara Oceans uncertainty spectra ($n = 87$). This weighting improved the relative median error (e_{median}; Table 2) by an average of 22% across all values of $a_{gaus}(\lambda_i)$.

The decomposition returns amplitudes associated with each Gaussian ($a_{\text{gaus}}(\lambda_i)$) and NAP ($a_{\text{NAP}}(\lambda)$) function. We multiplied the retrieved amplitudes by the original component functions and summed them to generate the retrieved spectra (e.g. "Sum of Gaussian and NAP functions", Fig. 2). The sum of the Gaussian components only, i.e. excluding the function representing $a_{\text{NAP}}(\lambda)$, is assumed to represent the phytoplankton absorption spectrum ($a_\phi(\lambda)$). However, we recognize that NAP is not perfectly modeled by a decreasing exponential with the exponent defined to be -0.01 nm^{-1}. In addition, non-pigmented material in phytoplankton, e.g. cytoplasm and cell wall materials, may absorb similarly to $a_{\text{NAP}}(\lambda)$ (Aas, 1996).

2.4. Derivation of pigment–absorption relationships

We compared the computed amplitudes of each Gaussian function (in absorption units of m^{-1}) to HPLC pigment concentrations (in units of mg m^{-3}) to identify correlations at specific wavelengths. A non-parametric statistical analysis (Spearman's rank correlation coefficient, ρ) is used to test the relationship between HPLC pigment concentrations and retrieved phytoplankton peak absorption values. Since we assume the HPLC pigment concentrations to be "truth", we regress the y-axis data ($a_{\text{gaus}}(\lambda_i)$) against the x-axis data (HPLC pigment concentration) using type-I linear least-squares best fit. The fit is calculated for each log normalized $a_{\text{gaus}}(\lambda_i)$ and individual pigment (denoted as pigment$_j$) pair:

$$\log\{a_{\text{gaus}}(\lambda_i)\} = A_{ij} + B_{ij}\log[\text{pigment}_j]. \tag{4}$$

This relationship can be manipulated to solve for pigment concentration:

$$[\text{pigment}_j] = \{a_{\text{gaus}}(\lambda_i)/\exp(A_{ij})\}^{1/B_{ij}}. \tag{5}$$

The coefficients A_{ij} and B_{ij} (Table 2) describe the relationship between phytoplankton absorption at the ith peak inverted from in situ particulate absorption spectra for the jth pigment, and the HPLC-derived concentrations (HPLC$_j$). Eq. (5) provides the pigment concentration obtained from the decomposed Gaussian line height. We evaluate the goodness of fit for this inverted pigment concentration ([pigment$_j$]) by computing the relative median errors of all 210 match-up points using:

$$e_{\text{median}} = (\text{median}((\text{abs}([\text{pigment}_j] - \text{HPLC}_j))/HPLC_j)) * 100 \tag{6}$$

where for 50% of the data, the error in pigment concentration prediction is less than the e_{median} value. Note that using type-I regression and error estimates as in Eq. (6) assumes HPLC to be error free.

When comparing HPLC pigment concentrations with absorption peaks, we use the following definitions for each chlorophyll: total chlorophyll *a* (TChl *a*) = chlorophyll *a* + divinyl chlorophyll *a* + chlorophyllide *a*; total chlorophyll *b* (TChl *b*) = chlorophyll *b* + divinyl chlorophyll *b*; and chlorophyll *c* (Chl *c*) = chlorophyll *c1* + chlorophyll *c2*. We chose not to include chlorophyll *c3* in the Chl *c* sum due to differences in the absorption peaks of pigment-specific absorption spectra of Chl *c3* relative to Chl *c1* and Chl *c2*. We use combined, weighted values of TChl *b* and Chl *c* when comparing HPLC pigment concentrations to the absorption peak at 454 nm ($a_{\text{gaus}}(454)$) to account for absorption by both TChl *b* and Chl *c* at that wavelength. The equation of the weighted sum is: $(0.03 * \text{TChl}b + 0.07 * \text{Chl}c)/0.05$, with values for weighting based on Bricaud et al. (2004) pigment-specific absorption spectra.

The carotenoid pigments are grouped by similarities in pigment specific absorption spectra; photosynthetic carotenoids (PSC) are represented in this study by 523 nm and the pigments 19′-hexanoyloxyfucoxanthin + fucoxanthin + 19′-butanoyloxyfucoxanthin + peridinin, and the photoprotective carotenoids (PPC) are represented by 492 nm and the pigments α-carotene + β-carotene + zeaxanthin + alloxanthin + diadinoxanthin. The photosynthetic pigment α-carotene has been included in the PPC group due to the HPLC analysis, which reports α-carotene and β-carotene together as one value. Given the similarity in absorption spectra of the pigments found in each of the two groups, it is not possible with the current method to separate the presence of the different pigments in each of the PPC and PSC groups.

3. Method evaluation

3.1. Absorption and pigment correlations

We found strong correlations when comparing the three major chlorophyll pigments (chlorophylls *a*, *b*, and *c*) with wavelengths of peak absorption for each chlorophyll (Fig. 3, Table 2). e_{median} values range from 30% to 57% for all chlorophyll and carotenoid pigment predictions (Table 2). There is no improvement in the prediction of TChl *a* concentration compared to a prediction of TChl *a* using the method of line-height magnitude at 676 nm (Boss et al., 2013). Significant correlations are also found between the photosynthetic carotenoids (PSC) and absorption coefficients at 523 nm, and between the photoprotective carotenoids (PPC) and absorption coefficients at 492 nm (Fig. 5, Table 2).

One pigment that is not reported by HPLC analysis in our dataset is phycoerythrin, which is found in the cyanobacteria *Synechococcus* and *Trichodesmium*, as well as in *Cryptophytes*. Phycoerythrin has a unique absorption peak in the orange region of the visible spectrum, at approximately 550 nm. An analysis of residuals between measured particulate absorption spectra and the summed component functions resulting from the least squares inversion showed the presence of a peak at 550 nm (not shown). A map of the a_{gaus}(550 nm):a_{gaus}(675 nm) ratio for the Tara Oceans expedition shows higher ratios (indicating relatively higher amounts of phycoerythrin within the ensemble of phytoplankton pigments) in the major oceanic subtropical gyre regions and the productive Patagonian shelf region (Fig. 4).

We evaluated the importance of the unsmoothing (Section 2.2) by computing the decomposition on the spectra prior to unsmoothing. Five of the eight chlorophyll correlations (Fig. 3; ρ values in Table 2) were improved by 1.4%–7.5% when employing the unsmoothing. Unsmoothing also improves the correlations for the PSC pigments by 5.6%. Although the improvements are not large, the effect of the filter factors introduces a systematic bias that reduces the magnitudes of spectral features, most notably the TChl *a* absorption peak at ~675 nm. We recommend using the unsmoothing although the effects are not always significant since this removes a known instrumental bias.

3.2. Pigment ratios

In addition to error estimates of inverted pigment concentrations, we also compare inverted pigment concentration ratios (this section) and pigment-specific absorption values (Section 3.3) to those from the literature as an evaluation of our method. We found high co-linearity between modeled phytoplankton absorption, $a_{\text{gaus}}(\lambda_i)$ at all wavelengths (ρ values $=$ 0.76 or higher). Despite this co-linearity, which indicates that all phytoplankton pigments vary with each other to some extent, the ratios between individual pigments and TChl *a* using either peak absorption values (e.g. Fig. 4) or inverted pigment concentrations provide information on the relative concentration of different pigments to TChl *a*, which can be used to identify the presence of different phytoplankton types (Higgins and Mackey, 2000). We applied the decomposition method to the entire Tara Oceans dataset (binned to 1 km^2 spatial resolution; 69,944 global data points) and applied Eq. (5) (Section 2.4) to calculate inverted pigment concentration ratios for TChl *b*, Chl *c*, PPC, and PSC, each relative to TChl *a* (at 675 nm) (Table 3; Fig. 6).

3.3. Pigment specific absorption

Phytoplankton absorption and pigment concentration co-vary with one another, but are modulated by pigment packaging. The pigment-specific phytoplankton absorption coefficient (denoted $a_\phi^*(\lambda)$) is defined as the absorption per unit concentration of a given pigment (m^2 mg^{-1}). The value of $a_\phi^*(\lambda)$ varies due to pigment packaging, which has the effect of decreasing the absorption efficiency of phytoplankton with increasing cell size or increasing pigment concentration for a given cell size (Duysens, 1956; Kirk, 1975; Morel and Bricaud, 1981). The packaging effect can introduce errors in the predicted pigment concentrations. Linear best-fit calculations on log-transformed data (Eq. (4)), however, already include some of the change in pigment-specific absorption as a function

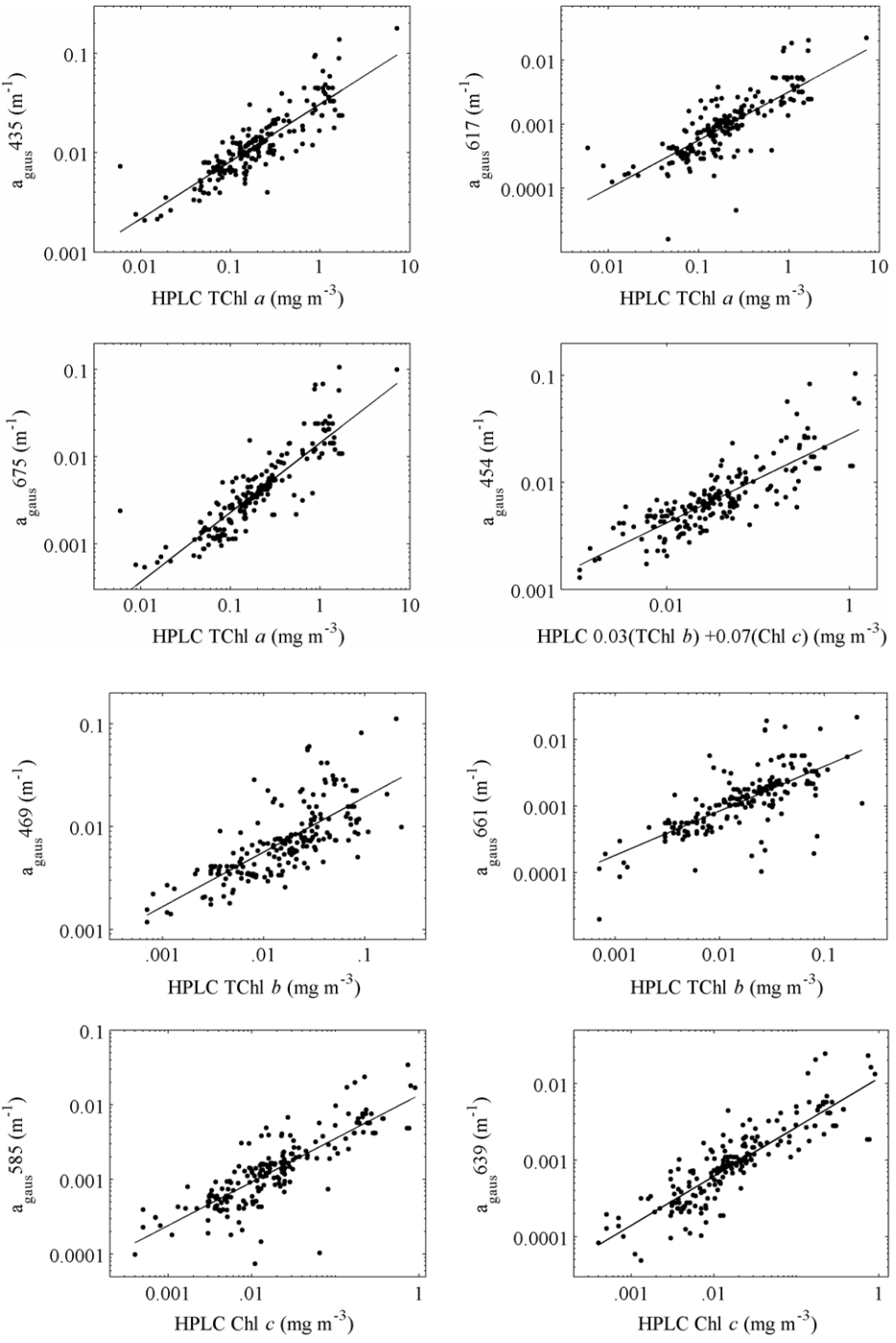

Fig. 3. HPLC-measured chlorophyll concentrations (*x*-axes) vs. magnitudes of Gaussian peak absorption (*y*-axes) at eight different wavelengths (note that plot 2 in row 2 uses $a_{gaus}(454)$ and the weighted sums of both TChl *b* and Chl *c*; see Section 2.4 for details). Best-fit lines show a first order linear regression performed on the log transforms of both datasets.

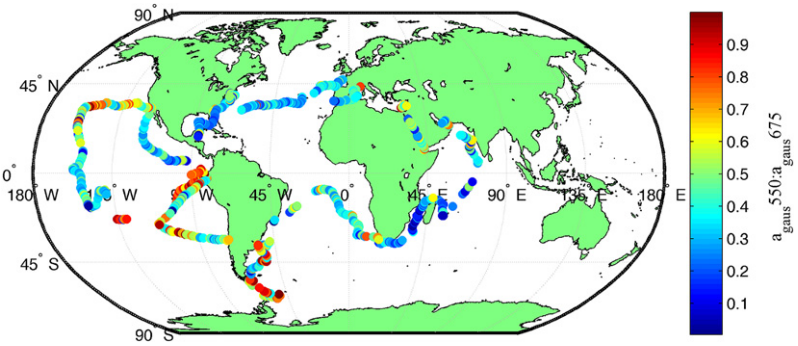

Fig. 4. Ratio of the 550 nm:675 nm Gaussian functions, representing absorption by phycoerythrin normalized to absorption by TChl *a*. Data points are from in situ absorption measurements made during the Tara Oceans expedition. Every 50th point is shown for ease of plotting (1,399 out of 69,944 total points). Data with a ratio >1 (9% of points) are considered outliers and are omitted from the figure.

Table 3
Median and range (95% confidence interval) values for inverted pigment concentration ratios to TChl *a* from this study and range of values from the literature. Ratio values calculated from the Tara Oceans expedition (1 km^2 binned; 69,944 points). Histograms of ratio values shown in Fig. 6.

Pigment ratio	Ratio median	Ratio range (95% confidence interval)	Ratio from literature
TChl *b*:TChl *a*	0.073	0.004–0.443	0–1.41[a,b,c]
Chl *c*:TChl *a*	0.101	0.010–0.314	0–0.532[a,b]
PPC:TChl *a*	0.363	0.164–0.995	0.05–1.4[a]
PSC:TChl *a*	0.379	0.060–2.247	0–1.8[a]

[a] Bricaud et al. (2004).
[b] Mackey et al. (1996).
[c] Descy et al. (2009).

of pigment concentration (which tends to correlate with cell size). Thus, some of the variations in $a_\phi^*(\lambda)$ are accounted for if packaging co-varies with concentration and if $a_\phi^*(\lambda)$ is calculated using the equation: $a_\phi^*(\lambda) = A[\text{pigment}]^{B-1}$ (Bricaud et al., 1998). We calculated $a_\phi^*(\lambda)$ using the equation: $a_\phi^*(\lambda) = a_{\text{gaus}}(\lambda_i)/[\text{HPLC}_j]$, to allow for comparison to previously published values, and report median values and range (95% confidence interval) for all 210 match-up data points (Table 4).

4. Summary and recommendations for future work

In the evaluation of our approach, we found that both our pigment concentration ratios (Table 3; Fig. 6) and $a_\phi^*(\lambda)$ values (Table 4) are in general agreement with previously published values. Consistency in ratios of inverted pigment concentrations with values from the literature suggests that the application of decomposition of absorption spectra measured in situ may provide information on relative pigment concentrations, which can be used to identify different phytoplankton types. Our values for PSC:TChl *a* are slightly higher than literature values, which may be a result of inaccurate removal of the NAP signal (an underestimated NAP signal would result in larger $a_{\text{gaus}}(\lambda_i)$ magnitudes, particularly in blue wavelengths). We currently have no direct way to evaluate our removal of the NAP signal from the particulate absorption spectra, as NAP data were not collected. The $a_\phi^*(\lambda)$ we found were mostly within the range of values found in the literature, with several median $a_\phi^*(\lambda)$ values higher than previously published values.

The approach presented here can be expanded upon in a number of different ways. The residuals of the least-squares inversion may contain information about pigments that are not well represented by the currently used Gaussian functions. Additionally, retrievals of phycoerythrin could possibly be tested using flow-cytometric and/or fluorescence data. Since multiple pigments within each of the two major carotenoid groups (PPC and PSC) are well correlated with the absorption peaks 492 nm

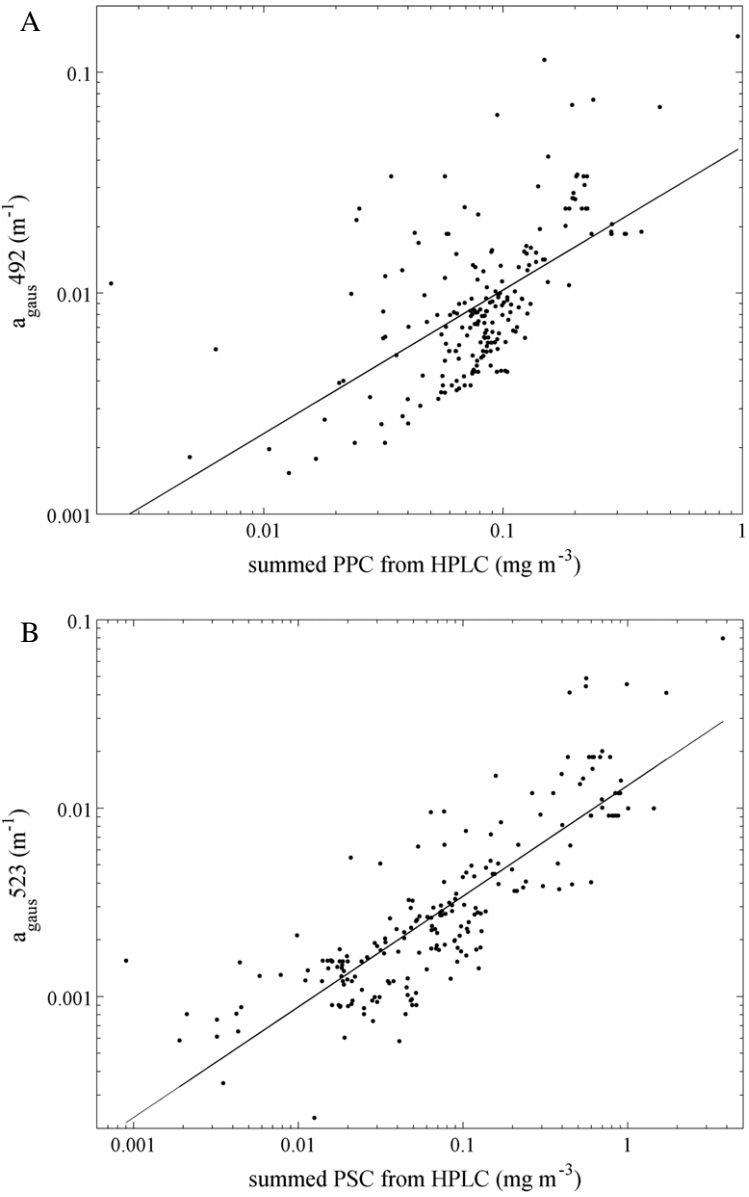

Fig. 5. HPLC-measured carotenoid pigment concentrations vs. modeled phytoplankton absorption at 492 nm (A) and 523 nm (B). (A) shows the summed photoprotective carotenoids (PPC) measured using HPLC: α-carotene + β-carotene + zeaxanthin + alloxanthin + diadinoxanthin. (B) shows the summed photosynthetic carotenoids (PSC) measured using HPLC: 19′-hexanoyloxyfucoxanthin + fucoxanthin + 19′-butanoyloxyfucoxanthin + peridinin. Best-fit lines show a first order linear regression performed on the log transforms of both datasets.

and 523 nm (respectively), it is challenging to estimate specific pigment values using absorption spectra alone beyond the PPC and PSC groupings. Therefore, combining absorption information with other parameters such as size information (from attenuation spectra (Boss et al., 2001) or the absorption spectra itself (Organelli et al., 2013)) and environmental conditions could allow more accurate prediction of some accessory phytoplankton pigments.

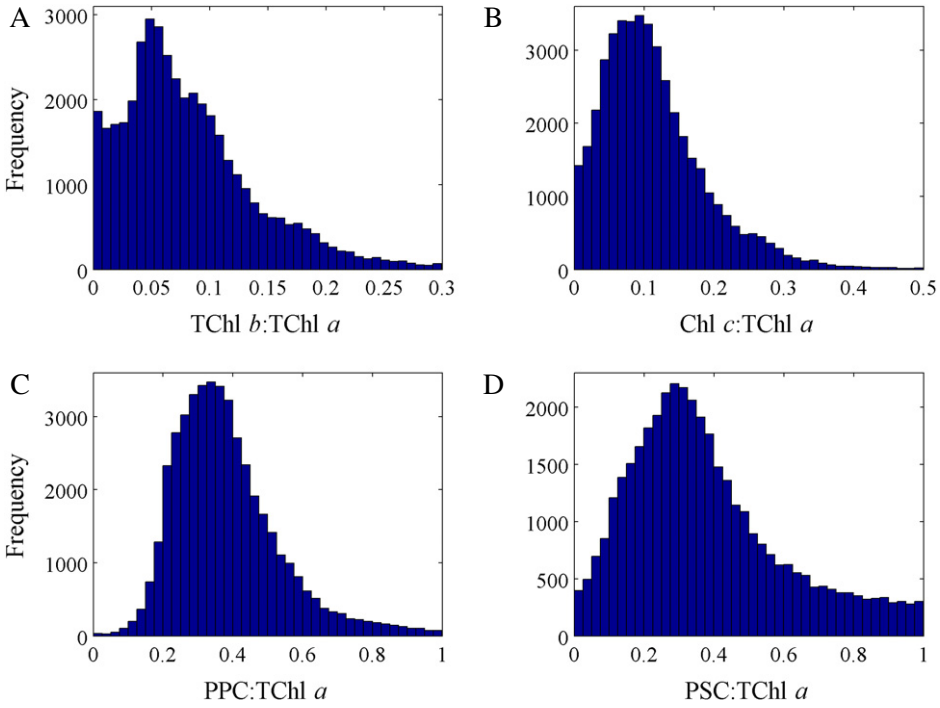

Fig. 6. Distributions of inverted phytoplankton pigment concentrations for TChl *b*, Chl *c*, PPC, and PSC, each normalized to TChl *a*. TChl *a* is inverted from the 675 nm peak, TChl *b* is inverted from the 661 nm peak, Chl *c* from the 639 nm peak, PPC from the 492 nm peak, and PSC from the 523 nm peak. See Section 2.4, Eq. (5) for details on the calculation of pigment concentrations. Data shown in these plots are from the entire Tara Oceans ship track, binned to 1 km^2 spatial resolution (69,944 data points). 3.9%, 0.7%, 2.5%, and 15.3% of data points have pigments ratios >0.3, 0.5, 1, and 1 in plots A, B, C, and D respectively, and are omitted from the figure.

Table 4
Median and range (95% confidence interval) of values for pigment-specific absorption ($a_\phi^*(\lambda)$) at each absorption wavelength from this study, and range of values from the literature. $a_\phi^*(\lambda)$ is defined as the amount of absorption per unit pigment concentration: $a_\phi^*(\lambda) = a_{gaus}(\lambda_i)/[\text{HPLC}_j]$.

Wavelength (nm)	Pigment (s)	$a_\phi^*(\lambda)$ median	$a_\phi^*(\lambda)$ range (95% confidence interval)	$a_\phi^*(\lambda)$ from literature
435	TChl *a*	0.065	0.015–0.165	0.034–0.09[a,b,c]
617	TChl *a*	0.005	0.001–0.018	0.003–0.004[a,c]
675	TChl *a*	0.019	0.007–0.065	0.02–0.035[a,c]
454	0.03(TChl *b*) + 0.07(Chl *c*)	0.208	0.013–1.66	N/A
469	TChl *b*	0.440	0.056–2.179	0.033–0.24[a,c]
661	TChl *b*	0.072	0–0.408	0.005-0.007[a,c]
585	Chl *c*	0.073	0–0.420	0.006–0.019[a,b,c]
639	Chl *c*	0.051	0.010–0.247	0.008–0.02[a,b,c]
492	PPC	0.097	0.049–0.797	0.035–0.055[a,b,c]
523	PSC	0.035	0.010–0.243	0.028–0.035[a,c]

[a] Bricaud et al. (2004).
[b] Lohrenz et al. (2003).
[c] Bidigare et al. (1990).

5. Conclusions

Obtaining information on the presence of phytoplankton pigments can be used to qualitatively describe the phytoplankton present in a given water body, which is desired to study phytoplankton

population dynamics and their relationship with their environment. The method presented here demonstrates the value of hyperspectral particulate absorption spectra measured in situ for detection and quantification of the concentration of chlorophylls a, b and c. Besides in-line systems, such measurements of particulate absorption spectra have been obtained on moored platforms (Slade et al., 2010). Our ability to estimate the pigment concentrations of chlorophylls b and c and their ratios to chlorophyll a from particulate absorption spectra provides information that is currently not attainable using in situ fluorometry (Chekalyuk et al., 2012; Chekalyuk and Hafez, 2013). The dataset of match-up points used in this study span five years and a wide range of locations throughout the world's oceans, which implies that the $a_{\mathrm{gaus}}(\lambda_i)/[\mathrm{pigment}_j]$ relationships are relatively well constrained in space and time. In-line systems, such as that used during the Tara Oceans expedition (Slade et al., 2010), can record large quantities of data with relatively low effort, thus providing a more comprehensive view of phytoplankton ecology than is currently available using laboratory-based phytoplankton absorption measurements.

Acknowledgments

Thanks to the scientists and crew of the Tara Oceans expeditions, in particular M. Picheral and S. Searson for their efforts in the collection of quality AC-S spectra. Thanks to W. Slade and J. Loftin for installation of the instrument and management of logistics, and L. Taylor and T. Leeuw for the processing of all raw Tara Oceans AC-S data. Thanks to M. Ouhssain for the extraction and HPLC analysis of Tara Oceans pigment samples. We sincerely thank the commitment of the people and the following institutions and sponsors who made this singular expedition possible: CNRS, EMBL, Genoscope/CEA, UPMC VIB, Stazione Zoologica Anton Dohrn, UNIMIB, ANR, FWO, BIO5, Biosphere 2, agnès b., the Veolia Environment Foundation, Region Bretagne, World Courier, Cap L'Orient, the Foundation EDF Diversiterre, FRB, the Prince Albert II de Monaco Foundation, Etienne Bourgois, the Tara Foundation teams and crew. Tara Oceans would not exist without the continuous support of the participating institutes (see http://dx.doi.org/10.1371/journal.pbio.1001177). This is contribution no. 12 of the Tara Oceans Expedition 2009–2012. Funding for the collection and processing of the Tara Oceans AC-S dataset was provided by NASA Ocean Biology and Biogeochemistry program under grants NNX11AQ14G and NNX09AU43G to the University of Maine.

Appendix

Note: The full script for decomposition of high-resolution particulate absorption spectra is available at: http://misclab.umeoce.maine.edu/software.php

Correcting filtered spectral data.

We let the measured absorption spectrum be given by $a_{\mathrm{meas}}(\lambda)$. The filter factors for the AC-S are given by $f(\lambda, \lambda')$ and can be defined by the following MATLAB script:

```
wavelength=.1:.1:799;
SIG1=(-9.845*10^-8.*currwvn.^3   +1.639*10^-4*currwvn.^2- 7.849*...
          10^-2*currwvn + 25.24) /2.3547;
    for i=1:max(size(currwvn));
        for jkl=1:max(size(wavelength));
            filtfunc(jkl,i)=(1/(sqrt(2*pi)*SIG1(i)))*...
                exp(-0.5*((wavelength(jkl)-currwvn(i))/SIG1(i)).^2);
        end
   end
```

Where "currwvn" is the array of wavelengths associated with the AC-S measurement.

The wavelength of nominal measurement is λ and λ' are the wavelengths near it that are allowed through the filter. The correction consists of convolving the measured data with the filter factors and assuming that the subsequent change is nearly the same as the change of the true spectrum when convolved with the filter factors.

If we have a true absorption spectrum given by $a_{\text{true}}(\lambda)$, we then get:

$$\int_{\lambda_{\min}}^{\lambda_{\max}} a_{\text{true}}(\lambda')f(\lambda,\lambda')d\lambda' = a_{\text{meas}}(\lambda). \tag{A.1}$$

Note that this is a simple matrix equation that in theory could be inverted directly. The data is not exact, however and a direct inversion leads to instabilities. We therefore developed an iteration method.

We can define the difference between $a_{\text{true}}(\lambda)$ and $a_{\text{meas}}(\lambda)$ as:

$$d_{\text{true}}(\lambda) = a_{\text{true}}(\lambda) - a_{\text{meas}}(\lambda). \tag{A.2}$$

We can now convolve Eq. (A.2) with the filter factors:

$$\int_{\lambda_{\min}}^{\lambda_{\max}} d(\lambda')f(\lambda,\lambda')d\lambda' = \int_{\lambda_{\min}}^{\lambda_{\max}} a_{\text{true}}(\lambda')f(\lambda,\lambda')d\lambda' - \int_{\lambda_{\min}}^{\lambda_{\max}} a_{\text{meas}}(\lambda')f(\lambda,\lambda')d\lambda'. \tag{A.3}$$

And, using Eq. (A.1), we get:

$$\int_{\lambda_{\min}}^{\lambda_{\max}} d(\lambda')f(\lambda,\lambda')d\lambda' = a_{\text{meas}}(\lambda) - \int_{\lambda_{\min}}^{\lambda_{\max}} a_{\text{meas}}(\lambda')f(\lambda,\lambda')d\lambda'. \tag{A.4}$$

We know $a_{\text{meas}}(\lambda)$ and we can calculate $\int_{\lambda_{\min}}^{\lambda_{\max}} a_{\text{meas}}(\lambda')f(\lambda,\lambda')d\lambda'$, hence we know

$$d'(\lambda) = \int_{\lambda_{\min}}^{\lambda_{\max}} d(\lambda')f(\lambda,\lambda')d\lambda'. \tag{A.5}$$

The correction applied to the AC-S assumes to first order (to start the iteration) that

$$d'(\lambda) \sim d(\lambda). \tag{A.6}$$

The first iterated spectrum thus consists of:

$$a_{\text{corrmeas}}1(\lambda) = a_{\text{meas}}(\lambda) - d'(\lambda).$$

We now repeat this and will converge on a spectrum for which

$$\int_{\lambda_{\min}}^{\lambda_{\max}} a_{\text{corrmeas}}(\lambda')f(\lambda,\lambda')d\lambda' = a_{\text{meas}}(\lambda). \tag{A.7}$$

When comparing Eq. (A.7) with Eq. (A.1) we see that

$$\int_{\lambda_{\min}}^{\lambda_{\max}} a_{\text{corrmeas}}(\lambda')f(\lambda,\lambda')d\lambda' = \int_{\lambda_{\min}}^{\lambda_{\max}} a_{\text{true}}(\lambda')f(\lambda,\lambda')d\lambda'. \tag{A.8}$$

Or,

$$\int_{\lambda_{\min}}^{\lambda_{\max}} [a_{\text{corrmeas}}(\lambda') - a_{\text{true}}(\lambda')]f(\lambda,\lambda')d\lambda' = 0. \tag{A.9}$$

This does not mean that the spectra are equal, only that when convolved with the filter factors they are equal. Any spectrum that when convolved with the filter factors is zero, cannot contain any data with higher frequencies than those that were filtered away.

References

Aas, E., 1996. Refractive index of phytoplankton derived from its metabolite composition. J. Plankton Res. 18 (12), 2223–2249.

Bidigare, R.R., Morrow, J.H., Kiefer, D.A., 1989. Derivative analysis of spectral absorption by photosynthetic pigments in the western Sargasso. Sea, J. Mar. Res. 47, 323–341.

Bidigare, R.R., Ondrusek, M.E., Morrow, J.H., Kiefer, D.A., 1990. In vivo absorption properties of algal pigments. Proc. SPIE 1302, 290–302.

Boss, E., Picheral, M., Leeuw, T., Chase, A., Karsenti, E., Gorsky, G., Taylor, L., Slade, W., Ras, J., Claustre, H., 2013. The characteristics of particulate absorption, scattering and attenuation coefficients in the surface ocean; contribution of the Tara Oceans expedition. Methods in Oceanography. http://dx.doi.org/10.1016/j.mio.2013.11.002.

Boss, E., Twardowski, M.S., Herring, S., 2001. Shape of the particulate beam attenuation spectrum and its relation to the size distribution of oceanic particles. Appl. Opt. 40, 4885–4893.

Bricaud, A., Claustre, H., Ras, J., Oubelkheir, K., 2004. Natural variability of phytoplanktonic absorption in oceanic waters: influence of the size structure of algal populations. J. Geophys. Res. 109, C11010.

Bricaud, A., Mejia, C., Blondeau-Patissier, D., Claustre, H., Crepon, M., Thiria, S., 2007. Retrieval of pigment concentrations and size structure of algal populations from their absorption spectra using multilayered perceptrons. Appl. Optics. 46 (8), 1251–1260.

Bricaud, A., Morel, A., Babin, M., Allali, K., Claustre, H., 1998. Variations of light absorption by suspended particles with chlorophyll a concentration in oceanic (case 1) waters: analysis and implications for bio-optical models. J. Geophys. Res. 103, 31033–31044.

Chekalyuk, A., Hafez, M., 2013. Next generation Advanced Laser Fluorometry (ALF) for characterization of natural aquatic environments: new instruments. Opt. Express. 21 (12), 14181–14201.

Chekalyuk, A., Landry, M., Goericke, R., Taylor, A.G., Hafez, M., 2012. Laser fluorescence analysis of phytoplankton across a frontal zone in the California Current ecosystem. J. Plankton Res. 34 (9), 761–777.

Dall'Olmo, G., Westberry, T.K., Behrenfeld, M.J., Boss, E., Slade, W.H., 2009. Significant contribution of large particles to optical backscattering in the open ocean. Biogeosciences 6, 947–967.

Descy, J.P., Sarmento, H., Higgins, H.W., 2009. Variability of phytoplankton pigment ratios across aquatic environments. Eur. J. Phycol. 44 (3), 319–330.

Duysens, L.N.M., 1956. The flattening of the absorption spectrum of suspensions, as compared to that of solutions. Biochim. Biophys. Acta 19, 1–12.

Higgins, H.W., Mackey, D.J., 2000. Algal class abundances, estimated from chlorophyll and carotenoid pigments, in the western Equatorial Pacific under El Nino and non-El Nino conditions. Deep-Sea Res. PT I. 47, 1461–1483.

Hoepffner, N., Sathyendranath, S., 1991. Effect of pigment composition on absorption properties of phytoplankton. Mar. Ecol. Prog. Ser. 73, 11–23.

Hoepffner, N., Sathyendranath, S., 1993. Determination of the major groups of phytoplankton pigments from the absorption spectra of total particulate matter. J. Geophys. Res. 98 (C12), 22,789–22,803.

Hooker, S.B., Heukelem, L.V., Thomas, C.S., Claustre, H., Ras, J., Schlüter, L., Clementson, L., van der Linde, D., Eker-Develi, E., Berthon, J.-F., Barlow, R., Sessions, H., Ismail, H., Perl, J., 2009. The Third SeaWiFS HPLC Analysis Round-Robin Experiment (SeaHARRE-3). National Aeronautics and Space Administration, Goddard.

Iturriaga, R., Siegel, D.A., 1989. Microphotometric characterization of phytoplankton and detrital absorption properties in the Sargasso Sea. Limnol. Oceanogr. 34, 1706–1726.

Johnsen, G., Samset, O., Granskog, L., Sakshaug, E., 1994. In vivo absorption characteristics in 10 classes of bloom-forming phytoplankton: taxonomic characteristics and responses to photoadaptation by means of discriminant and HPLC analysis. Mar. Ecol. Prog. Ser. 105, 149–157.

Karsenti, E., Acinas, S.G., Bork, P., Bowler, C., De Vargas, C., et al., 2011. A holistic approach to marine ecosystems biology. PLoS Biol. 9 (10), e1001177.

Kirk, J.T.O., 1975. A theoretical analysis of the contribution of algal cells to the attenuation of light within waters, II, spherical cells. New Phytol. 75, 21–36.

Kirkpatrick, G., Millie, D.F., Moline, M.A., Schofield, O., 2000. Optical discrimination of a phytoplankton species in natural mixed populations. Limnol. Oceanogr. 45, 467–471.

Lohrenz, S.E., Weidemann, A.D., Tuel, M., 2003. Phytoplankton spectral absorption as influenced by community size structure and pigment composition. J. Plankton Res. 25 (1), 35–61.

Mackey, M.D., Mackey, D.J., Higgins, H.W., Wright, S.W., 1996. CHEMTAX — a program for estimating class abundances from chemical markers: application to HPLC measurements of phytoplankton. Mar. Ecol. Prog.-Ser. 144, 265–283.

Millie, D.F., Schofield, O.M., Kirkpatrick, G.J., Johnsen, G., Tester, P.A., Vinyard, B.T., 1997. Detection of harmful algal blooms using photopigments and absorption signatures: a case study of the Florida red-tide dinoflagellate *Gymnodinium breve*. Limnol. Oceanogr. 42, 1240–1251.

Moisan, J.R., Moisan, T.A.H., Linkswiler, M.A., 2011. An inverse modeling approach to estimating phytoplankton pigment concentrations from phytoplankton absorption spectra. J. Geophys. Res. 116, C09018.

Moore, C., Bruce, E.J., Pegau, W.S., Weidemann, A.D., 1997. In: Ackleson, S.G. (Ed.), WETlabs ac-9: Field Calibration Protocol, Deployment Techniques, Data Processing, and Design Improvements, Ocean Optics XIII. In: SPIE Proceedings, Vol. 2963. International Society for Optical Engineering, pp. 725–730.

Morel, A., Bricaud, A., 1981. Theoretical results concerning light absorption in a discrete medium, and application to specific absorption of phytoplankton. Deep Sea Res. 28, 1375–1393.

Organelli, E., Bricaud, A., Antoine, D., Uitz, J., 2013. Multivariate approach for the retrieval of phytoplankton size structure from measured light absorption spectra in the Mediterranean Sea (BOUSSOLE site). Appl. Opt. 52, 2257–2273.

Ras, J., Uitz, J., Claustre, H., 2008. Spatial variability of phytoplankton pigment distributions in the Subtropical South Pacific Ocean: comparison between in situ and modelled data. Biogeosciences 5, 353–369.

Rhoades, B., Derr, A., Moore, C., Zaneveld, J.R., 2004. The AC-spectra, an instrument for hyperspectral characterization of inherent optical properties in natural waters. In: Ocean Optics XVII, Fremantle, Australia, October 25–29.

Slade, W., Boss, E., Dall'Olmo, G., Langner, M.R., Loftin, J., Behrenfeld, M.J., Roesler, C., Westberry, T.K., 2010. Underway and moored methods for improving accuracy in measurement of spectral particulate absorption and attenuation. J. Atmos. Ocean. Technol. 27 (10), 1733–1746.

Sullivan, J.M., Twardowski, M.S., Zaneveld, J.R.V., Moore, C., Barnard, A., Donaghay, P., Rhoades, B., 2006. The hyperspectral temperature and salinity dependencies of absorption by water and heavy water in the 400–750 nm spectral range. Appl. Opt. 45, 5294–5309.

Uitz, J., Claustre, H., Morel, A., Hooker, S.B., 2006. Vertical distribution of phytoplankton communities in open ocean: an assessment based on surface chlorophyll. J. Geophys. Res. 111, C08005.

Van Heukelem, L., Thomas, C.S., 2001. Computer-assisted high-performance liquid chromatography method development with applications to the isolation and analysis of phytoplankton pigments. J. Chromatogr. A 910, 31–49.

Westberry, T.K., Dall'Olmo, G., Boss, E., Behrenfeld, M.J., Moutin, T., 2010. Coherence of particulate beam attenuation and backscattering coefficients in diverse open ocean environments. Opt. Express. 18 (15), 15419–15425.